Chemistry with Element 106, Seaborgium – The Isotopes ^{265}Sg and ^{266}Sg.

M. Schädel [1], J. Alstad [4], M. Andrassy [8], W. Brüchle [1], R. Dressler [5], K. Eberhardt [2], B. Eichler [5], B. Fricke [13], H.W. Gäggeler [5,6], M. Gärtner [5], R. Günther [2], K.E. Gregorich [10], R. Heimann [2], D.C. Hoffman [10,11], S. Hübener [7], E. Jäger [1], D.T. Jost [5], B. Kadkhodayan [12,11], J.V. Kratz [2], D.M. Lee [10], R. Malmbeck [3], M. Mendel [2], R. Misiak [8], A. Nähler [2], Y. Nagame [14], J.P. Omtvedt [4], Y. Oura [14], W. Paulus [2], V. Pershina [13], F. Rocker [2], B. Schausten [1], E. Schimpf [1], D. Schumann [8], A. Seibert [2], G. Skarnemark [3], E. Sylwester [10], St. Taut [7], S. Timokhin [9], U. Tharun [2], P. Thörle [2], N. Trautmann [2], A. Türler [5], N. Wiehl [2], B. Wierczinski [10], G. Wirth [1], A. Yakuschew [9], S. Zauner [2]

[1] GSI, Darmstadt, [2] Universität Mainz, Mainz, [3] Chalmers University of Technology, Göteborg, [4] University of Oslo, Oslo, [5] Paul Scherrer Institut, Villigen, [6] Universität Bern, Bern, [7] FZ Rossendorf, Dresden, [8] Technische Universität Dresden, Dresden, [9] Flerov Laboratory of Nuclear Reactions, Dubna, [10] Lawrence Berkeley National Laboratory, Berkeley, [11] Glenn T. Seaborg Institute for Transactinium Science, Livermore, [12] Lawrence Livermore National Laboratory, Livermore, [13] Gesamthochschule Kassel, Kassel, [14] Japan Atomic Energy Research Institute, Tokai.

We have successfully performed the first experiments on *the chemistry of element 106, seaborgium (Sg).* Furthermore studies on *the production and decay of ^{265,266}Sg* were carried out. The main emphasis of our experimental program is to study the chemical properties of Sg, and to compare these with extrapolations in the Periodic Table and with predictions from relativistic calculations. In addition, our experiments add new information about increased nuclear stability in the region of deformed shell closure around N=162.

Recently, a Dubna-Livermore collaboration [1] has discovered the isotopes ^{266}Sg and ^{265}Sg as products from the ^{22}Ne on ^{248}Cm reaction. Half-lives between 2 s and 30 s were estimated from the measured α-energies [1]. These half-life estimates, together with cross sections of the order of 100 to a few hundred picobarns, made this reaction, and especially the isotope ^{265}Sg, a promising candidate to perform chemical studies on Sg.

Our first aim was (i) to identify the isotope ^{265}Sg, and possibly ^{266}Sg, after chemical separation, (ii) to obtain first information about the seaborgium chemistry, (iii) to get a first measurement of the half-lives of these isotopes, and (iv) to confirm the cross sections given in [1].

To optimize the chemical separation procedures for Sg a number of experiments have been performed with Mo and W, the lighter homologs of Sg, and with U as a hexavalent pseudo-homolog. In addition, tracer activities of Zr, Hf, and lanthanides were used to study the chemistry of the unwanted elements rutherfordium, Rf, (Z=104) and the actinides (see contributions to previous Scientific Reports).

All targets were prepared by electrodeposition techniques. First, we used targets of about 0.15 mg/cm^2 ^{248}Cm while the main experiments were carried out with a 0.95 mg/cm^2 ^{248}Cm target. During all experiments, the 153.8 MeV ^{22}Ne beam from the UNILAC was degraded in energy by a 2.67 mg/cm^2 Be vacuum-window, 0.65 mg/cm^2 N_2 cooling-gas, and the 2.65 mg/cm^2 Be target-backing before the ^{22}Ne entered the target at 122 MeV. The energy in the middle of the target was about 121 MeV. HIVAP calculations [2] show that the excitation function for the production of ^{265}Sg peaks in this energy region. Typically, the beam intensity was 3×10^{12} ions s^{-1}.

Nuclear reaction products, recoiling out of the target, were thermalized in a He-atmosphere of the recoil chamber and attached to aerosol particles in the gas. The flowing He transported the reaction products to one of our three experimental set-ups for chemical separations of Sg. The transport efficiency has been optimized and checked with ^{169}W produced in ^{22}Ne on ^{152}Gd. During the experiment we frequently monitored the transport efficiency by measuring transfer products from the ^{248}Cm target or from minor lighter element impurities in the target.

The **Automated Rapid Chemistry Apparatus, ARCA,** [3] enabled us to perform 5072 cyclic column liquid-chromatographic separations with a cycle- or collection time of 45 s (60 s in 1172 separations). KCl served as a cluster material in the He-jet to transport continuously the reaction products with a yield of 45 % within about 3 s to the collection site in ARCA. At the end-of-collection, 0.1 M HNO_3/ 5×10^{-4} M HF was used to wash all products onto a (8x1.6) mm cation exchange column filled with Aminex A-6, 17.5±2 μm. In this way, a Sg fraction was separated within 10 s. A typical elution curve ob-

tained with carrier-free W-tracer is shown in Fig. 1. A good separation is achieved from di- and trivalent actinides and group 4 elements, including Rf. Therefore, we can conclude that any decay of a Rf or No daughter, is evidence for the fact that Sg has passed through the chromatographic column.

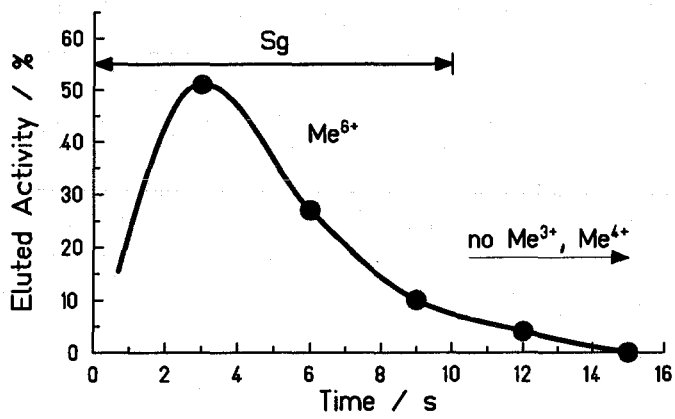

Figure 1: Elution curve for W-tracer modeling the Sg separation on ARCA.

After each separation, the solution, collected within 10 s, was rapidly dried to prepare a sample for α-spectroscopy (80 keV FWHM) and spontaneous fission (SF) fragment-energy measurements. The chemical yield was 80 %. A 6 min (8 min for experiments with 60 s cycle time) measurement started 38 s after the end-of-collection for each sample. The detection efficiency of the 450-mm^2 PIPS-detectors was 30 %. Energy, time, and detector information were stored for each event.

After a total dose of 2.31×10^{17} ^{22}Ne on the 0.15 mg/cm^2 and 5.48×10^{17} ^{22}Ne on the 0.95 mg/cm^2 thick target we observed two decay-chains with time-correlated α-α decays, see events # 1 and 2 in Table 1, which we assign to the decay of the ^{265}Sg-daughter ^{261}Rf into ^{257}No followed by the decay of this nuclide. These two event-chains have a significance of 97 % as the expected number of random correlations is 0.3. Most likely, the decay of ^{265}Sg was not seen because it decayed in the time interval between the end-of-separation and the start-of-measurement. It could have also escaped the detector.

We conclude, that, **for the first time, a chemical separation of element 106 was performed in aqueous solution.** Seaborgium shows a behaviour typical for a hexavalent element located in group 6 of the Periodic Table below Mo and W. Presumably, Sg forms anionic oxifluorides analog to the known complexes $[WOF_5]^-$ or $[WO_2F_3]^-$. The formation of other kinds of anionic or neutral complexes cannot be excluded at this point. Contrary to element 105 in group 5 [4], where a striking similarity of its chemical behaviour to that of the pseudo-group-5 element Pa was observed, these first experiments do not indicate a Sg behaviour similar to that of the pseudo-group-6 element U.

The **first experiment on element 106 in the gas-phase** was carried out with the **On-Line Gas Chemistry Apparatus, OLGA III** [5].

The chromatographic behaviour of Mo and W oxichlorides was investigated with $SOCl_2/Cl_2$ and $O_2/SOCl_2/Cl_2$ as chlorinating agents and carbon aerosols for the transport in the He-jet. The observed volatilities indicate the formation of MoO_2Cl_2 (adsorption enthalpy, ΔH_a= -90 kJ/mol) and WO_2Cl_2 (ΔH_a= -100 kJ/mol) which is less volatile, see Fig. 2.

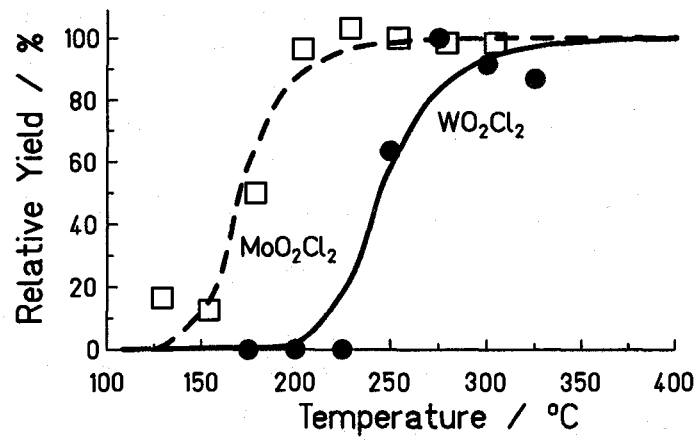

Figure 2: Relative yield of WO_2Cl_2 (dots) and MoO_2Cl_2 (squares) as a function of the temperature in OLGA together with Monte Carlo simulations (lines).

It was demonstrated with the short-lived isotopes ^{165}W-^{169}W from ^{20}Ne on ^{152}Gd test-reactions (i) that retention times of less than 10 s are achieved for W at isothermal temperatures above 275 °C, and (ii) that the separation from group 4 elements (Hf) is good. An additional partial pressure of $\leq$ 100 ppm O_2 did not change the volatility of W isotopes.

In the Sg experiments, OLGA was operated at 300-400 °C isothermal temperature in the gas-chromatography part of the column. 100 ml/min Cl_2 saturated with $SOCl_2$ and 2 ml/min O_2 were added as reactive agents. Products leaving the gas-chromatographic column after their specific retention time were attached to new aerosols in a recluster chamber and were transported through a capillary to the Rotating Wheel Multidetector Analyzer, ROMA.

Polypropylene foils of 60 μg/cm^2 were mounted on every second of 64 positions on the perimeter of the wheel to collect the products and rotate them in front of detectors for α- and SF-decay

energy-measurements. Seven pairs of 300-mm^2 PIPS-detectors (30% efficiency) were mounted along the perimeter of the wheel such that the angle between the collection position and the first detector pair and successive pairs was 11.25°.

In order to improve the significance of observed event chains, we implemented a parent-daughter mode for ROMA. The stepping time was 10 s in the parent mode which positioned catcher foils in front of the detectors. The registration of a triggering α in the bottom detector (through the catcher foil) – an indication that most likely the Sg-daughter nucleus (Rf) has recoiled into the top detector – initiated the wheel to move all sources away from the detectors for 2 min. In this daughter mode, hole positions in the catcher wheel were located between detector pairs. This allowed the clear identification of ^{265}Sg in two correlations observed in the daughter mode (event # 4 and 5 in Table 1). In addition, one very significant triple correlation (event # 3) was observed in the parent mode. We assign this sequence to the decay chain ^{265}Sg–^{261}Rf–^{257}No. Furthermore, a clear signature for the decay of ^{266}Sg and ^{262}Rf was registered with the 8.56 MeV α-decay followed 2.8 s later by a SF (event # 6).

Table 1: ^{265,266}Sg-events from 121 MeV ^{22}Ne + ^{248}Cm.

#	E(P) (MeV)	dt1 (s)	E(D) (MeV)	dt2 (s)	E(D) (MeV)	dt3 (s)
			ARCA			
1	–	–	8.24	33.5	8.22	67.4
2	–	–	8.26	22.7	8.10	8.2
			OLGA			
3	8.86	2.8	8.38	31.0	8.05	14.8
4	8.84	27.3	8.13	53.3	–	–
5	8.85	0.6	8.30	48.4	–	–
6	8.56	48.9	SF	2.8	–	–

E(P), E(D): parent(P) –, daughter(D) energies
dt1: time after end-of-collection
dt2: time after start-of-measurement (ARCA), or time after first α-event (OLGA)
dt3: time after 1st (ARCA) or 2nd (OLGA) α-event

From the observed α-decays we obtain with a 68 % confidence interval (c.i.) for
^{265}**Sg** : $\mathbf{T_{1/2} = (7.1 + 8.6/ - 2.5)}$ **s,**
$\sigma = \mathbf{(270 + 360/ - 170)}$ **pb,** and for
^{266}**Sg** : $\mathbf{T_{1/2} = (34 + 163/ - 15)}$ **s,**
$\sigma = \mathbf{(50 + 115/ - 41)}$ **pb.**

Combining the ARCA and OLGA results considerably reduces the range of possible $T_{1/2}$- and σ-values; see Fig. 3 for ^{265}Sg. These results are in good agreement with half-lives deduced from the observed α-energies in the discovery experiment [1] and with the cross sections, which were reported with an uncertainty of a factor ≈3. The measured cross sections are somewhat higher than the ones calculated with HIVAP [2], but with the present error bars this is not a significant effect.

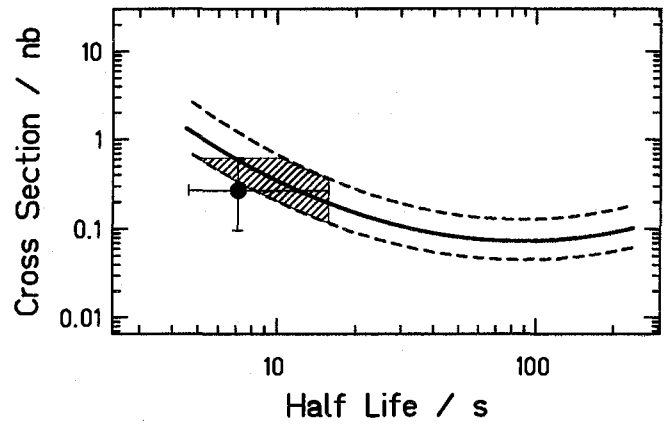

Figure 3: Cross section of ^{265}Sg (dot) from the OLGA experiment in comparison with the results from the ARCA experiment (solid line) with a 68 % c.i. (dashed lines). The error bars (68 % c.i.) reflect the statistical error. The dashed region indicates the area of possible $T_{1/2}$ – and σ – values that are compatible both with OLGA- and ARCA results.

We have measured 9 SF-events in the ARCA experiment. This is still compatible (95% c.i.) with the background, which, at least partially, may originate from a small ^{256}Fm contamination. Calculating an upper limit for the cross section of a SF-branch in ^{266}Sg and comparing this with the cross section obtained from the α-decay observed in OLGA yields an upper limit of 80 % for the SF-branch in ^{266}Sg. The partial half-life for SF-decay deduced from this branching ratio is in the region calculated by [6], see Fig. 4, and by [7] for the so called "Old Path". It is more than a factor 10^5 longer than the calculated half-life for the so called "New Path" [7] which was expected to dominate.

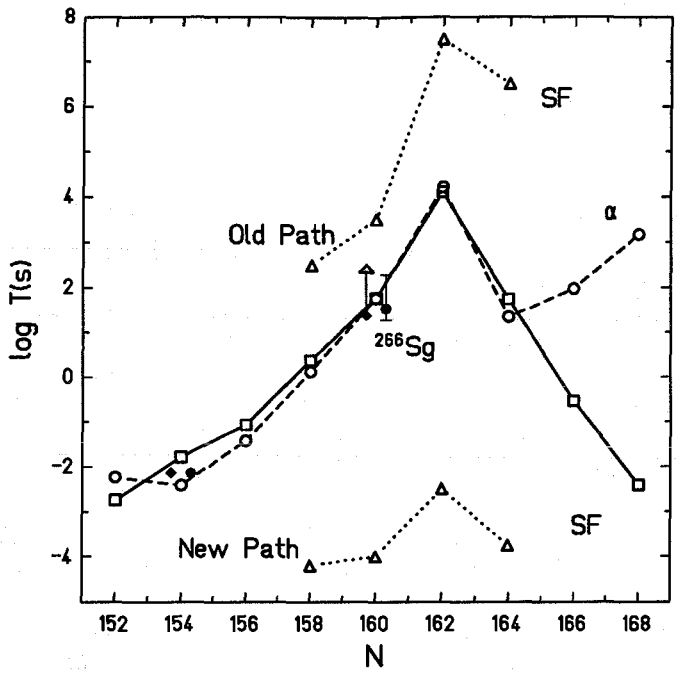

Figure 4: Measured (solid symbols) and calculated partial half-lives (open circles (α) and squares (SF) [6], open triangles (SF) [7]) for Sg isotopes.

Our chemical results show that Sg forms a volatile oxichloride-complex at 300-400 °C when Cl_2, saturated with $SOCl_2$, and small amounts of O_2 are present. Thermodynamic calculations indicate that SgO_2Cl_2 is formed in analogy to the known WO_2Cl_2. This agrees with the expected behaviour from an extrapolation in group 6 of the Periodic Table [8] and with theoretical calculations [9].

The centrifuge system **SISAK-3** [10] was used to extract continuously Sg from an aqueous solution into an organic phase. In this phase, time-correlated α- and SF-events were measured on-line with a liquid scintillation counting (LSC) system.

In previous experiments, it was shown that homologs of Sg can be extracted from an unbuffered 1 M α-hydroxyisobutyric acid (α-HIB) solution. The extractant was 0.046 M trioctylamine (TOA) dissolved in toluene which contains dimethyl-POPOP and naphthalin as scintillator. The group 4 homologs of Rf remain in the aqueous phase [11].

The LSC detection method provides an α-energy resolution of $\approx$ 300 keV (FWHM). In most cases this is sufficient to distinguish between different α-emitters. Nearly 100 % detection efficiency is achieved with this technique.

Two types of detector cells have been used: (i) a spherical cell made of opaque quartz (4 ml volume) which was placed in a semispherical teflon reflector to couple it optically to the photomultiplier tube (PMT), and (ii) a teflon cell ($\approx$ 7 ml) with a meander-like structure. The teflon cell was covered with an opaque quartz disk, and was coupled to the PMT with a cylindrical teflon reflector. The final detector system consisted of three consecutive units which allow half-life estimations. Events were listed and analyzed with respect to energy, pulse shape and the time difference between two successive events. Correlations between successive α-α- or α-SF-event were used to identify even very rare decay events. Pulse shape discrimination (PSD) and pile-up rejection was applied to suppress background events caused by β- and γ-radiation.

In our search for correlated α-SF-events, to identify the decay of ^{266}Sg, the observed number of events was within the expected range for random correlations due to the low effectivity of PSD for SF-events.

To increase the detection efficiency for α-α-α-correlations in the $^{265}Sg\rightarrow$ $^{261}Rf\rightarrow$ $^{257}No\rightarrow$ decay chain, the detection system was operated in such a mode where a trigger event in the 8.8 MeV region stopped the flow through the cell. This cell remained in this "daughter-mode" for 2 min to wait for the decay of daughter nuclei. Due to a relatively high β/γ background and a Po contamination, a number of random triple correlations resulted yielding a detection limit of about 1 nb for the interesting and most sensitive half-life region around 10 s. Work is in progress to improve the sensitivity by factors of 10-20 in forthcoming experiments.

References

[1] R. Lougheed et al., J. Alloy Comp. 213/214, 61 (1994), and Yu. A. Lazarev et al., Phys. Rev. Letters 73, 624 (1994).

[2] W. Reisdorf and M. Schädel, Z. Phys. A - Hadrons and Nuclei 343, 47 (1992).

[3] M. Schädel et al., Radiochim. Acta 48, 171 (1989).

[4] J.V. Kratz et al., Radiochim. Acta 48, 121 (1989).

[5] H.W. Gäggeler et al., Nucl. Instr. and Methods in Phys. Research A309, 201 (1991).

[6] A. Sobiczewski et al., J. Alloy Comp. 213/214, 38 (1994).

[7] P. Möller, J.R. Nix, J. Alloy Comp. 213/214, 43 (1994).

[8] B. Eichler, H.W. Gäggeler, Lab. f. Radio- und Umweltchemie, PSI, Annual Report 1993, p.40.

[9] V. Pershina et al., contribution to this Scientific Report.

[10] J. Alstad et al., J. Radioanal. Nucl. Chem. 189, 133 (1995).

[11] B. Wierczinski et al., Radiochim. Acta 69, 77 (1995).

Complex Formation of Element 106 in Aqueous HCl and HF+HCl Solutions

V. Pershina and B. Fricke
Fachbereich Physik, Universität Kassel, D-34109 Kassel, Germany

In preliminary experiments to study the complex formation of element 106, various systems were tried in order to find proper conditions to separate the lighter analogs, Mo and W. The best conditions were found for the mixture of 0.05 HCl and 10^{-3} HF acids as an aqueous phase, which allows separation of Mo and W from group 4 ions and trivalent actinides by using the cation exchange resins [1]. Some good conditions were found for the separation of W from Mo and from some other elements (Zr, Nb, U) in the extraction from aqueous HCl solutions at high concentrations by different organic extragents [2].

In the present work we have studied the complex formation of the lighter analogs of 106, Mo and W, and of U in HCl and HF+HCl solutions on the basis of an analysis of numerous experimental data. Using results of our DS DVM calculations [4cd] we predicted behavior of the 106-complexes in the process of extraction from these solutions by organic solvents.

In aqueous 2-6 M HCl solutions predominant species of Mo and W are monomeric MO_2Cl_2, between 6 and 12 M - $MO_2Cl_2^{3-}$ and above 12 M the formation of $MO_2Cl_4^{2-}$ starts. MO_2Cl_2 were shown to exists in the form of the adduct, $MO_2Cl_2(H_2O)_2$, favoring the octahedral structure with *cis*-oxy-ligands [3]. In organic solutions the adducts have the same form, having organic molecules in the coordination sphere, e.g. *cis*-$MO_2Cl_2(OEt_2)_2$. In aqueous HF solutions Mo and W are supposed to form $[MO_2F_3(H_2O)]^-$ or $(MO_2F_n)^{(n-2)-}$ complexes at different concentrations [3]. Uranium forms various $UO_2F_n^{z-n}$ complexes. In HF+HCl solutions, at low HCl concentrations (and/or higher HF) predominant species of Mo and W are the oxyfluoride complexes. At higher HCl molarities the neutral and oxychloride complexes are predominant.

DS DVM calculations [4] confirmed the full analogy between $106O_2Cl_2$ and MO_2Cl_2 (M=Mo and W). Thus, one can assume formation of the same type of complexes for element 106 in HCl solution as those of Mo and W. The obtained electronic configuration of 106 ($d^{4.1}s^{0.5}$ [4c]) in $106O_2^{2+}$ shows a ds-hybridization, defining a *cis*-position of the oxygen atoms.

Results of the extraction of the Mo, W and U species from aqueous HCl solutions on the one hand and from HF solutions on the other hand by different organic media have shown opposite trends in the distribution coefficients: D(U)>D(Mo)>D(W) and D(U)<D(Mo)<D(W), respectively [5,6] (see also Fig. 1 for HF+HCl solutions, 1M HF [6]). This must be connected with two different extraction mechanisms. In the first case, the mechanism of the adduct formation is valid:

$$2(R_3NHCl) + MO_2Cl_2(H_2O)_2 \rightarrow MO_2Cl_2(R_3NHCl)_2 .$$

The process of the molecule transfer (ΔG_t) in this case, and finally of the extraction, is defined by a strength of the dipole-dipole interaction of the $MO_2Cl_2(H_2O)$ species with water molecules. The values of dipole moments for the compounds under study obtained as a result of the DS DVM calculations [4c] are shown in Table 1.

Preliminary calculations [4d] have shown that this is also the case for $MO_2Cl_2(H_2O)_2$. Thus, the sequence in the values of the dipole moments of MO_2Cl_2 will define a reverse sequence in the distribution coefficients of these compounds. The expected position of D(106) will be below that of W (Fig. 1).

Table 1. Dipole moments for MO_2Cl_2 (M=Mo, W, 106 and U)

	MoO_2Cl_2	WO_2Cl_2	$106O_2Cl_2$	UO_2Cl_2
μ (*D*)	1.04	1.35	1.83	0

A pseudoanalog within the actinides, uranium, in aqueous HCl solutions at intermediate concentrations is known to form $UO_2Cl_2(H_2O)_2$, with a linear structure of the uranyl ion UO_2^{2+}, in contrast to the d-element compounds, thus having no dipole moment. A linear structure is defined by a fd-hybridisation (U: $f^{3.1}d^{1.7}s^{0.09}$ in UO_2^{2+} [7]). The absence of the dipole moment for the uranium compound explains its superior extractability.

In HF or HF+HCl solutions the anion exchange takes place:

$$R_3NHCl + MO_2F_3^- \rightarrow R_3NH(MO_2F_3) + Cl^- .$$

Here, the work of transfer will be determined by a size of the extracted species. Nevertheless defining species at very low HF concentration is a difficult task still to be solved.

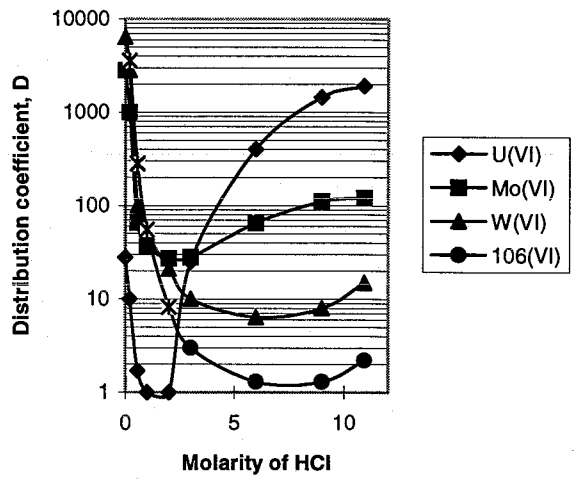

Fig. 1. Adsorption of group 6 elements and U from HCl+HF solutions (preliminary estimates for 106 are shown by stars).

References

[1]. Schumann, D. et al. GSI Scientific Report 1993, p. 241.
[2]. Becker, H. U. Ph. D. Thesis, Mainz 1994, pp.100, 127.
[3]. Griffith, W. P. J. Chem. Soc. (A), 1967, 675.
[4]. (a) Pershina,V. et al. J. Phys. Chem. 1994, 98, 6468, (b) ibid 1995, v. 99, p. 144; (c) ibid, in press; (d) in preparation;
[5]. Caletka, R. J. Radioanal. Nucl. Chem., 1990, 142, 373.
[6]. Kraus, K. A. et al. J. Am. Chem. Soc. 1955, 77, 3972.
[7]. Pershina, V. et al. Russ. J. Inorg. Chem. 1990, 35, 1178.

The Electronic Structure and Thermochemical Stability of Group 6 Dioxide Dichlorides, MO_2Cl_2 (M=Cr, Mo, W, and Element 106)

V. Pershina, T. Bastug, and B. Fricke
Fachbereich Physik, Universität Kassel, D-34109 Kassel, Germany

Halides and oxyhalides of element 106 and its analogs are the species, volatility of which is to be studied experimentally by using the gas-phase chromatography technique [1]. Relativistic MO calculations [2,3] have shown that both the pure halide of element 106, $106Cl_6$, and the oxide tetrachloride, $106OCl_4$, will decompose at high temperatures by analogy with $MoCl_6$ and $MoOCl_4$ transforming into compounds of Mo(V). In this work we present results of the Dirac-Slater Discrete-Variational calculations of the electronic structure of the group 6 dioxide dichlorides, MO_2Cl_2 (M = Cr, Mo, W, and element 106), and their analysis with respect to the stability of the compounds towards thermal decomposition. In Tables 1 and 2 the Mulliken analysis data and obtained on their basis estimates of the bond energies (see ref [4] for the procedure) are presented. In Fig. 1 energies of the highest occupied MO (HOMO) and lowest unoccupied MO (LUMO) are shown for these compounds in comparison with those of group 6 $MOCl_4$.

Table 1. Effective charges, Q_M, overlap populations, OP, and dipole moments, μ , for MO_2Cl_2

	MoO_2Cl_2	WO_2Cl_2	$106O_2Cl_2$
Q_M	1.03	1.08	0.97
OP(M=2O)	1.07	1.38	1.48
OP(M-2Cl)	0.64	0.86	0.85
OP(tot)	1.72	2.23	2.34
μ, *D*	1.04	1.35	1.83

Trends in Q_M, OP and the metal-ligand bond energies are reminiscent of those for the group 6 $MOCl_4$. The trend in the energies of the LUMO is however different: the LUMO in $106O_2Cl_2$ is lowered relative to that in WO_2Cl_2 (Fig.1). (This was also not the case for the MCl_6 series of the compounds). A resulting decrease in the value of the energy gap is indicative of the diminished stability of the +6 oxidation state of 106 in $106O_2Cl_2$ relative to W(6+) of WO_2Cl_2.

Table 2. Estimates of the bond energy in MO_2Cl_2, eV

	MoO_2Cl_2	WO_2Cl_2	$106O_2Cl_2$
ΔH_{diss} (M=O)	6.86	7.75	7.45
ΔH_{diss} (M-Cl)	3.64	4.05	3.45
ΔH_{diss} (mol)	21.08	23.52	21.6 - 23.0

The fact that the dioxide dichlorides of Mo and W are more stable than the corresponding oxide tetrachlorides cannot be accounted for by a higher covalency of their metal-ligand bonds: the partial OP data for the M=O and M-Cl bonds and corresponding bond energies are very similar in MO_2Cl_2 and $MOCl_4$ (see Table 2 and Tables 1 and 3 in ref 3). Obviously, a much higher stability of MoO_2Cl_2 and WO_2Cl_2 is explained by much higher values of their ΔE, which are 2.46 and 1.89 eV larger than those of $MoOCl_4$ and $WOCl_4$, respectively. Much larger values of the energy gaps prevent the metals from being easily reduced, the process which normally accompanies the thermal dissociation of the group 6 halides and oxyhalides. Taking this into account, single molecules of WO_2Cl_2 and $106O_2Cl_2$ should also be more stable than $WOCl_4$ and $106OCl_4$, though their M-Cl bond strengths are similar.

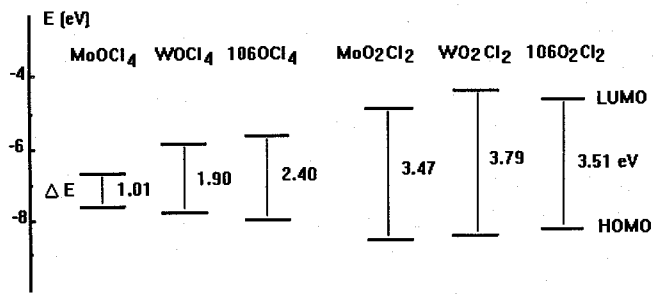

Fig. 1. Energies of the highest occupies (HOMO) and lowest unoccupied (LUMO) MO and the values of energy gaps between them for group 6 $MOCl_4$ and MO_2Cl_2.

The decomposition of WO_2Cl_2 and $106O_2Cl_2$ would occur only when at least two molecules, needed for the reaction

$$2MO_2Cl_2\,(g) \Rightarrow MO_3\,(s) + MOCl_4\,(g)\,, \quad (1)$$

are produced simultaneously, with the enthalpies of the reaction (1) for W and 106 compounds being estimated as -25.56 and -70.60 kcal/mol, respectively. This is, however, not the case for the one-atom-at-a-time production rates of these elements. The enthalpy of formation, $\Delta H_f(106O_2Cl_2)$, was estimated as -121.72 kcal/mol, which is less negative than the value for WO_2Cl_2 of -163.96 kcal/mol.

A lower volatility of the dioxide dichlorides compared to that of the oxide tetrachlorides is explained: i) by slightly lower covalency of the former compounds and ii) by much higher values of the dipole moments. A lower volatility of WO_2Cl_2 compared to that of MoO_2Cl_2 is a result of a larger dipole moment of the former compound. One can expect the lowest volatility of $106O_2Cl_2$ in comparison with the lighter analogs due to the largest value of the dipole moment, making its interaction with the surface of the chromatography column the strongest.

References.

[1] Gäggeler, H. W. et al. GSI Scientific Report 1991, ISSN 0174-0814, p. 321; Türler, A. et al. PSI Annual Report 1993, p.43.
[2] Pershina, V. and Fricke, B. J. Phys. Chem. 1994, 98, 6468.
[3] Pershina, V. and Fricke, B. J. Phys. Chem., 1995, 99, 144.
[4] Pershina, V. et al. J. Chem. Phys., 1992, 97, 1116.

Heavy Ion Induced Modification of Superconductors

G. Wirth, E. Jäger, M. Schädel, E. Schimpf
GSI, Darmstadt: for HTS collaborations

(1) W.S. Seow[a], R.A. Doyle[a], A.M. Campbell[a], G. Balakrishnan[b], K. Kadowaki[c]
[a] IRC, Univ. of Cambridge, [b] Dep. of Phys., Univ. of Warwick, [c] Nat.Res.Inst.,Sengen,Tsukuba-Shi
(2) F. Hillmer, P. Haibach, U. Frey, Th. Kluge, H. Adrian
Inst. für Physik, Univ. Mainz

The structure and dynamics of magnetic flux lines in high-T_c superconductors (HTS) is a rich field of basic and interesting physics [1] that can be investigated by the introduction of crystal defects. Heavy ions are a powerful tool to enable the controlled introduction of different types of crystal defects by the choice of the ion species and ion energy. Optimum pinning sites are continuous amorphous cylinders with a diameter comparable to the coherence length of a few nanometer. These columnar defects can be created with very heavy ions. The introduction of correlated disorder by heavy ions is not only attractive because of the optimum pinning strength, but also a well defined defect density can be achieved. The orientation of the heavy ion tracks relative to the crystal axis and an external magnetic field gives access to angle resolved measurements. These investigations are also relevant for applications because of the main material intrinsic current limiting process of dissipation by the motion of flux lines.

In collaboration with groups from several laboratories and applying different techniques various aspects of magnetic flux lines in superconductors and their interaction with heavy ion induced defects are investigated using GSI facilities. Both, thin films and crystals of different high-T_c materials are investigated. Besides the measurements of the superconducting properties a characterization of the defects by high resolution transmission electron microscopy and X-ray diffraction gives some necessary input for an understanding of the pinning mechanism. The distribution of magnetic field at a microscopic level within a material can be obtained by neutron diffraction and muSR. We did first irradiations aimed to investigate the microscopic flux structure within the bulk of high-T_c superconductors after the creation of columnar defects in thick crystals using Uranium ions at SIS energies. First preliminary results indicate, that defects can be created passing the crystals with a thickness of a few hundred mikrometers and magnetic scattering of neutrons from flux lines pinned to the defects can be observed (spokesperson: E.M. Forgan, Univ. of Birmingham).

The substantial results from all HTS collaborations can not be shown in this short report. Instead, two examples will demonstrate the influence of correlated disorder on the flux line structure in a layered Bi-compound HTS superconductor. These experiments look for anisotropic pinning effects taking advantage of the well defined orientation and density of correlated disorder introduced by heavy ions into HTS samples.

When a magnetic field is applied along the c-axis of the anisotropic HTS $Bi_2Sr_2CaCu_2O_8$ (BSCCO) two-dimensional pancake vortices are formed instead of the usual vortex lines in 3D superconductors. This means, that the vortex 'lines' are extremely sensitive to thermal fluctuations resulting in flux cutting and dissipation. Heavy ion irradiation may increase the apparent tilt modulus C_{44} and the vortices pinned to the columnar tracks then may behave as well-coupled flux lines. It raises the question of the relative contributions of Lorentz-force driven and other sources of dissipation related to the low dimensionality. When both the magnetic field and transport current are applied parallel to each other, the Lorentz force disappears and one obtains a force free configuration. Therefore, c-axis transport measurements on as produced and heavy ion irradiated crystals with different doses and directions of irradiation were performed (1). Significant enhancement in the irreversibility

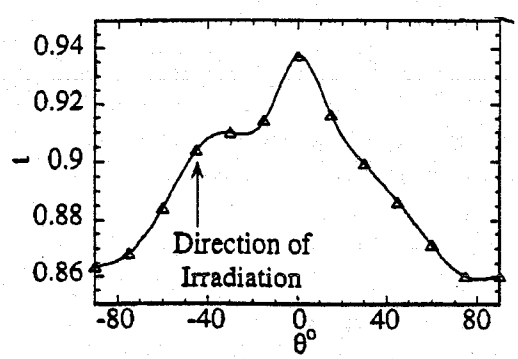

Fig. 1: Scaled irreversibility temperature for an applied field of 0.4T. The crystal was irradiated at 45° with B_Φ=0.4T.

lines of the irradiated crystals is observed, and even

in the force free geometry. Extracted irreversibitity temperatures $T_{irr}(B,\Theta)$ show, that there is locking in of vortex lines with large accomodation angles after irradiation. Fig.1 shows the first observation of such uniaxial enhancement from transport measurements on BSCCO crystals. This suggests, that vortices in heavy ion irradiated crystals of BSCCO are well coupled rather then consisting of independent pancakes when B is applied parallel to the correlated disorder.

In order to further elucidate the line-like nature of these vortices, measurements using the flux transformer geometry have been made (1). In fig.2 the orientation of the tracks and external magnetic field are illustrated schematically. It is clear that the bottom voltage converges to the same value as the top voltage for B parallel while this does not occur when the field is anti parallel to the defects. Since matched voltages mean that the flux line velocity at the top and bottom faces of the crystal are the same, this strongly suggests well correlated vortex line motion which implies that vortices display 'line-like' features after heavy ion irradiation.

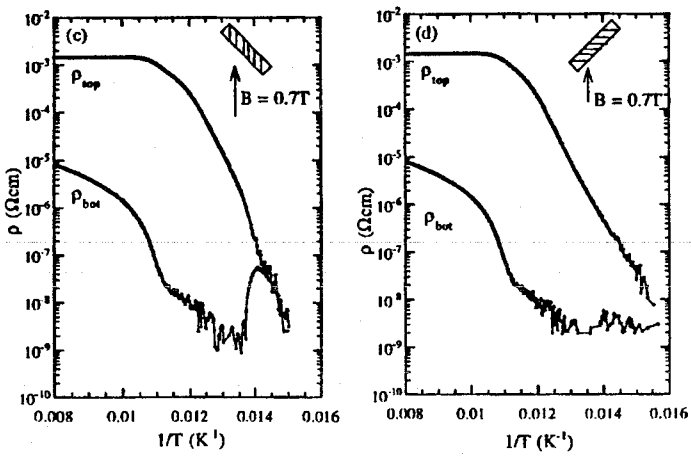

Fig. 2: Top and bottom apparent resistivities of the flux transformer geometry at B=0.7T (same crystal as in fig.1).

Of course it is an interesting question whether this strong effect of the columnar defects on the flux line structure also will lead to an anisotropic enhancement of the critical current density determined from transport measurements. In order to reach the critical current density for a broad range of temperatures and magnetic fields with reasonable measuring currents, thin film samples are best suited. To look for anisotropic pinning one has to compare different samples irradiated at various angles with respect to the film c-axis. But the preparation of high quality films with identical characteristics is difficult. This experimental problem was solved and four samples with practically the same T_c and resistive transitions were obtained by striplines patterned close to each other on one film (2). By shielding, only one strip was irradiated with heavy ions at a time.

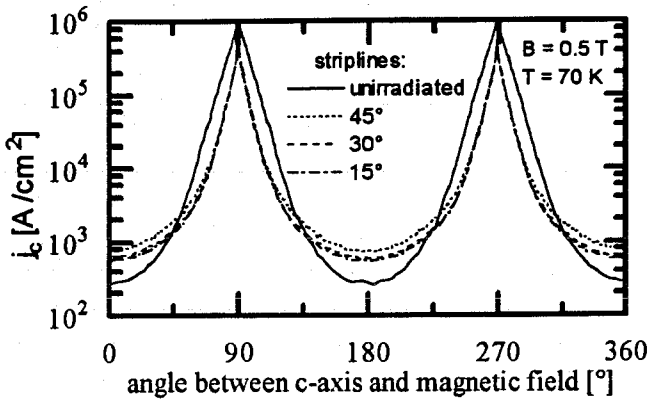

Fig. 3: Critical transport current density in the applied field of 0.5T. Three of the four striplines patterned on one film were irradiated with B_Φ=1T at angles given in the figure.

Fig.3 displays the angular dependence of the transport critical current density. The striplines were irradiated with a dose equivalent B_Φ=1T at angles as given in the figure. The directions of magnetic fields and irradiations are always in a plane perpendicular to the transport current. Obviously there is no uniaxial enhancement at angles with the applied magnetic field parallel to the columnar defects. Nevertheless, for magnetic fields close to B_Φ and parallel to the film c-axis (in fig.3 = 0°/180°) the critical current density is enhanced. A closer inspection of the data shows an enhancement of the critical current density independent of the direction of the columnar defects, when the projected densities of vortices and defects are equal in the a-b plane perpendicular to the film c-axis.

It remains to be clarified, why the line-like structure of the vortices after the introduction of correlated disorder with columnar defects, as it was observed with crystals in flux tranfomer geometry and by uniaxial enhancement of the irreversibility line, is not visible in the transport critical current density of thin films. Either material intrinsic differences or an influence of the measured quantities itself may give an explanation.

References

[1] Vortices in high temperature superconductors: G.Blatter, M.V.Feigel'man, V.B.Geshkenbein, A.I.Larkin, V.M. Vinokur, Rev. Mod. Phys. 66(4), 1125 (1994)

Sorption Behaviour of W, Hf, Lu, U, and Th Radionuclides on Ion Exchange Resins from HCl/H_2O_2 Containing Aqueous Solutions

D. Schumann [1], M. Andrassy [1], H. Bruchertseifer [5], W. Brüchle [4], R. Misiak [3], H. Nitsche [1], A.F. Novgorodov [2], M. Schädel [4], B. Schausten [4]
[1] TU Dresden, [2] JINR Dubna, [3] IFJ Krakau, [4] GSI Darmstadt, [5] PSI Villigen

In [1] we reported on chemical studies for the separation of subgroup IV elements and lanthanides from W and Mo by use of cation exchange from diluted HCl/HF containing aqueous solutions as model experiments for the separation of element 106. First applications with the ARCA III apparatus showed that a good sorption of Hf onto the cation exchange resin can be obtained using the proposed solutions, but the system is partially influenced by hydrolysis if very diluted solutions are used [2]. Unfortunately, the concentration of HCl and HF cannot be increased, because sorption of subgroup IV elements would take place only incompletely [1, 2]. Hence, the system is very sensitive to small changes of concentration, and adsorption on surfaces due the hydrolytic processes can take place in some cases. Therefore, it would be desirable to develop chemical systems with a higher content of acid to suppress hydrolysis completely. W and Mo are known to form stable anionic complexes with H_2O_2 in acid solutions up to 10 M HCl [3]. Hf and lanthanides form positively charged compounds [4]. This makes the system possibly suitable for the separation of subgroup VI elements from IV ones. In some cases similarities of transactinide elements with the corresponding actinides must be expected. Therefore, in the present work the behaviour of U and Th was taken into consideration. Experimental details are given in [5].

Sorption of Hf, Lu, W, and Th on cation and anion exchangers

In figure 1 the lg D values of Hf, Lu, W, Th, and U on DOWEX 50x8 and DOWEX 1x8 as a function of HCl concentration in the presence of 0.5 vol.% H_2O_2 are plotted. Suitable H_2O_2 concentrations were determined in preliminary studies. It can be seen that W shows strong sorption on the anion exchanger over the whole range of HCl concentrations, while the sorption is very weak on the cation exchanger at concentrations higher than 0.05 M HCl. This refers to the formation of anionic compounds. At concentrations lower than 0.05 M HCl W shows also sorption on DOWEX 50x8, probably caused by hydrolytic processes. Hydrolysis influences also the sorption of Hf which is known to hydrolyze strongly in weak acid solution [6]. While it is completely sorbed on DOWEX 50x8 over the whole HCl concentration interval it shows also strong sorption on the anion exchanger for concentrations lower than 0.1 M HCl. With increasing HCl concentration the sorption on DOWEX 1x8 decreases but the strong sorption on DOWEX 50x8 remains. From this, a positively charged complex can be proposed which is partially hydrolysed in weak acid solutions. This, similar to Hf, sorbed on the cation exchanger and, following, behaves like a typical tetravalent element. On the cation exchanger it shows a higher distribution coefficient, which is probably caused by formation of neutral compounds. Lu as the model element for trivalent lanthanides and actinides shows strong sorption on DOWEX 50x8 and no sorption on the anion exchange resin over the whole range of HCl concentrations (fig. 1).

From these results follows that good conditions for the separation of W from tri- and tetravalent elements can be found at HCl concentrations between 0.1 and 1.0 M.

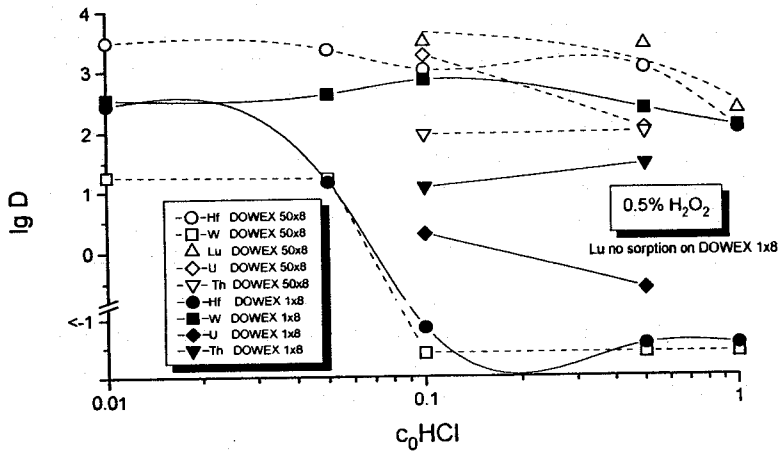

Fig. 1: lg D values of Lu, Hf, W, Th, and U on DOWEX 50x8 and DOWEX 1x8 in dependence on HCl concentration at 0.5 vol.% H_2O_2.

Sorption of U on cation and anion exchangers

Under the conditions described above U does not behave similar to subgroup VI elements but shows strong sorption on the cation exchanger resin (fig. 1). Following, in the case that element 106 is more U-like, the HCl/H_2O_2 system is not suitable for first separation experiments because element 106 will remain completely on the cation exchange column. Nevertheless it can be used in further experiments for determining similarities of the chemical properties of element 106 either with W or with U after a preliminary separation of actinides and element 104.

References

[1] D. Schumann et al., Radiochim. Acta 1995, in print
[2] R. Günther et al., GSI Scientific Report 1994, p. 302
[3] J. Korkisch, Handbook of Ion Exchange Resins, CRC Press, Inc. Boca Raton, Florida 1989
[4] J.A. Connor, E.A.V. Ebsworth, Advances in Inorg. Chem. and Radiochem. **6** (1964) 279-381
[5] D. Schumann et al., Radiochim. Acta **69** (1995) 35
[6] C.F. Baes, R.E. Mesmer, The Hydrolysis of Cations, John Wiley and Sons, New York, (1976) 1076, p. 412

This work was supported by BMFT, Germany.

Thermochromatography of Heavy Actinides at High Temperatures

St. Taut, S. Hübener, H. Nitsche (FZ Rossendorf), B. Eichler (PSI Villigen), H. W. Gäggeler (Universität Bern),
M. Schädel, E. Jäger, W. Brüchle (GSI Darmstadt)

Characterization of metallic properties of actinides is a good approach to obtain information about their electronic state. Since actinides beyond Es are available only in trace amounts, very few experimental physicochemical data exist for these elements.

The fact that macroscopic sublimation enthalpies generally correlate to adsorption enthalpies, which can be derived from thermochromatographic deposition temperatures, opens the opportunity to search for quantitative data with this method even for the last actinides, which can only be measured by atom-at-a-time chemistry.

The experimental setup used in this work provides high temperatures, which were not obtainable until now. Thus, in preparation for future experiments with elements beyond Fm, a series of thermochromatographic data from earlier experiments [1] could be completed.

For our experiments we used a commercial gradient oven with 1600 K at the starting position. The columns with an inner diameter of 4 mm were inserted in a Ta support tube inside the oven, because the quartz tubes, used in previous experiments, do not withstand the high temperature. To prevent oxidation of the Ta tube it was flushed with He from the outside. Helium was also used as carrier gas with a velocity of 30 cm/s. The gases were purified from water and oxygen with a molecular sieve and a Ti getter, respectively.

The actinides under study were obtained from the heavy actinide fractions of Sg chemistry experiments, carried out at the UNILAC accelerator of the GSI Darmstadt with the $^{248}Cm + ^{22}Ne$ reaction. [2]

A nitric acid actinide solution was evaporated in a Ta boat and a small piece of La was added as a reductant. The boat was brought in starting position and heated for 30 minutes.The nuclide distribution along the thermochromatographic column was determined afterwards by alpha counting.

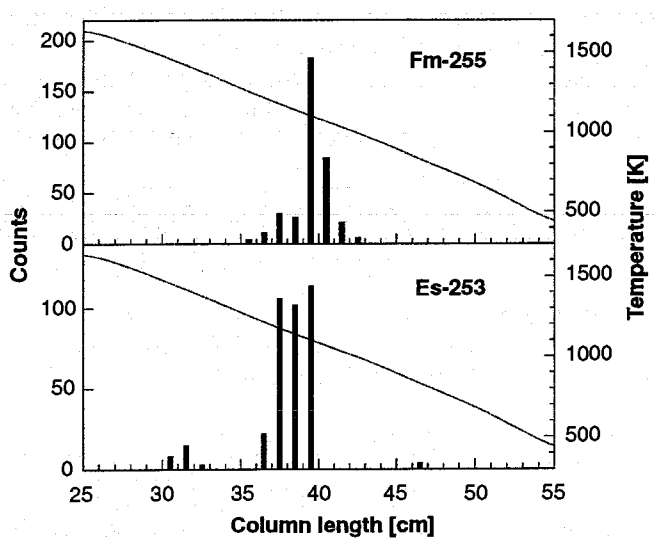

Fig. 1: Thermochromatogram of ^{253}Es and ^{255}Fm on a V column

Fig. 1 shows a typical chromatogram: the activity distribution of ^{253}Es and ^{255}Fm on a V column. To derive adsorption heats from the deposition temperatures the program TECRAD [3] was used.

Using the semi-empirical MIEDEMA method it is possible to calculate adsorption heats theoretically. Tab. 1 summarizes the experimental deposition temperatures, adsorption heats and the calculated adsorption heats [4].

Actinide	Column	Deposition Temp. [K]	Adsorption Enthalpy [kJ/Mol] This Work	Lit. [1]	Calc. M(II) [4]
Cf	Nb	1360	-343		-297
	Ta	1378	-348		-361
	V	1180	-299		-340
	Mo	1274	-322		-339
Es	Nb	1180	-299	-290	-228
	Ta	1337, 1162*	-338, -294*		-294
	V	1142	-289		-274
	Mo	1274	-322		-274
Fm	Nb	1142	-289	-270	-224
	Ta	1162	-294	-280	-280
	V	1103	-280		-263
	Mo	1142	-289	-290	-262

Tab. 1: Deposition Temperatures, Sublimation and Adsorption Enthalpies of Actinides; * 2 Peaks

As expected the deposition temperatures of Cf, Es and Fm differ from each other reflecting the tendency from metallic tri- to divalency in the second part of the actinide series. Thus, both chemical separation and characterization are possible.

Cf exhibits on Nb and Ta its position between the trivalent and divalent actinides. Surprising is its rather low adsorption enthalpy on V in comparison with Nb and Ta.

In contrary to the results, obtained by direct measurement of vapor pressures in [5] we can clearly see differences in the metallic properties of Es and Fm, especially on Mo.

The authors wish to express appreciation to K. E. Gregorich and N. Trautmann for providing the ^{248}Cm targets. This work was supported by both BMBF, contract 06DR666I(4)/1 and DFG, contract Hu642/1-1.

[1] Hübener, S., et. al.
J. All. Comp. **213[214** (1994), 429

[2] Schädel, M. et. al
GSI Scientific Report 1995, in preparation

[3] Funke, H. et. al.
Annual Report Institute of Radiochemistry,
Report No. FZR-43, (1993), 53

[4] Eichler, B.
in preparation

[5] Haire, R. G. et. al.
J. Chem. Phys. **91** (1989), 7085

Monte Carlo Simulation of Reaction Gas Chromatography of Group 6 Elements

A. Vahle[1], S. Hübener[1], R. Dressler[2], B. Eichler[2], A. Türler[2]
[1]Forschungszentrum Rossendorf, [2]Paul Scherrer Institut, Villigen, Switzerland

Gas chromatographic techniques have proven to be well suited to study kinetics and thermodynamics of desorption-adsorption processes of trace amounts. For this reason isothermal on-line gas chromatography is a favored technique for studying the chemical properties of the heaviest elements available only in quantities of single, short-lived atoms. However, the data of chromatography experiments cannot provide direct evidence of the species involved and hence the basic processes determining the chromatographic transport. Indirect evidence is possible, if data predicted on the basis of thermodynamic arguments and model calculations correspond with experimental results.

Monte Carlo calculations have been used to simulate the transport of volatile species through a gas chromatographic column for the case of reversible adsorption as basic process [1],[2]. Experimental data like the elution yield of isothermal gas chromatography and thermochromatograms were reproduced very well.

The chromatographic transport of group 6 elements in the O_2-$H_2O_{(g)}$/$SiO_{2(s)}$-system is governed by the surface reactions dissociative chemisorption and associative desorption as basic processes (M = Cr, Mo, W):

$$MO_2(OH)_{2\,(g)} \underset{\text{assoc. desorption}}{\overset{\text{diss. chemisorption}}{\rightleftharpoons}} MO_{3\,(ads)} + H_2O_{\,(g)} \qquad (1)$$

For this kind of chromatography we use the term reaction gas chromatography in order to distinguish from „normal" gas chromatography characterized by the transport of species with the same chemical state in the adsorbed and gaseous state [3].

In Monte Carlo simulations of chromatography the differences in the basic processes have to be considered. Therefore the adsorption residence time τ_a has to be defined. In the case of reversible adsorption τ_a is defined by the Frenkel equation and the period of oscillations of the adsorbed species perpendicular to the surface τ_0 has to be entered as variable [1],[2]. In the special case of reaction gas chromatography of group 6 elements in the O_2-$H_2O_{(g)}$/$SiO_{2(s)}$-system τ_a is determined mainly by the kinetics of the rate controlling associative desorption reaction and the collision probability of water molecules with the adsorbate, respectively. We define τ_a by a Frenkel-type equation and operate with a pseudo-period of oscillations τ_0^* evaluated approximately from Eq. (2) [1]:

$$\tau_0^* = \sqrt{\frac{2\pi \cdot M}{R \cdot T}} \cdot \frac{c^\circ_{ads}(MO_3)}{c_{gas}(H_2O)} \cdot e^{\frac{\Delta S^\circ_{diss.ads}}{R}} \qquad (2)$$

The term was obtained assuming that the volatile species $MO_2(OH)_2$ is desorbed immediately, $t_r >> t_{ads}$, p = 1 atm and

$$\frac{4}{d} \cdot \frac{c^\circ_{ads}(MO_3)}{c_{gas}(H_2O)} \cdot e^{\frac{-\Delta H^\circ_{diss.ads}}{R \cdot T}} \cdot e^{\frac{\Delta S^\circ_{diss.ads}}{R}} >> 1.$$

[1] t_r = retention time, M = mol mass of the transported species in the gaseous phase, R = gas constant, T = Temperature, c°_{ads} (MO_3) = standard concentration of MO_3 in the adsorbed state = $2{,}679 \cdot 10^{19}$ cm^{-2}, c_{gas} (H_2O) = concentration of H_2O in the gaseous phase, $\Delta S^\circ_{diss.ads}$ = standard entropy of dissociative adsorption, $\Delta H^\circ_{diss.ads}$ = standard enthalpy of dissociative adsorption, t_{ads} = total adsorption residence time

Values of τ_0^* can vary immensely. However, they are higher than those of τ_0 (10^{-12} - 10^{-14} s).

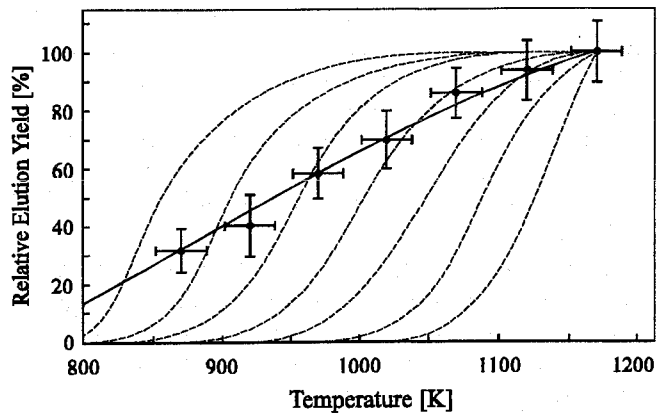

Fig. 1: Relative elution yield of ^{169}W as a function of the column temperature in isothermal on-line gas chromatography: experimental data and calculated yield curves
$p(H_2O)$ = 780 Pa, $v_0(He)$ = 1 l·min^{-1}, $v_0(O_2)$ = 0.5 l·min^{-1}
The solid line was calculated by the Monte Carlo method assuming transport via reaction (3) with $\Delta S^\circ_{diss.ads}$ = -41 J·mol^{-1}·K^{-1} and $\Delta H^\circ_{diss.ads}$ = -41 kJ·mol^{-1}. The dashed lines were calculated by the Monte Carlo method assuming reversible adsorption with $\Delta H^\circ_{diss.ads}$ = -180 kJ·mol^{-1} to -240 kJ·mol^{-1} in steps of 10 kJ·mol^{-1}.

In Fig. 1 experimental elution yields of ^{169}W are compared with results of Monte Carlo simulations. The dashed lines were obtained for different values of ΔH°_{ads} presuming reversible adsorption as basic reaction. None of these curves can reproduce the experimental data. The solid line was calculated assuming that tungsten is transported via reaction (3):

$$WO_2(OH)_{2\,(g)} \leftrightarrow WO_{3\,(ads)} + H_2O_{\,(g)} \qquad (3)$$

The shape of this calculated yield curve reproduces the experimental data very well. $\Delta H^\circ_{diss.ads}$ was determined to be -41 kJ·mol^{-1} and corresponds with the value of -25 ± 31 kJ·mol^{-1} expected for reaction (3) from thermodynamic considerations.

The elution yield depends less on column temperature than in the case of reversible adsorption. For this reason a significant increase of the elution yield can only be obtained if the temperature is risen extremely.

An increasing partial pressure of water in the carrier gas results in an increase of the elution yield, too. The retention time will be diminished due to the rising number of effective collisions.

Acknowledgements

These studies were supported by the BMBF of the FRG under contracts 06 DR 101 D and 06 DR 666 I(4)/1.

References

[1] I. Zvara, Radiochim. Acta 38, 95 (1985)

[2] A. Türler et al., PSI Condensed Matter Research and Material Sciences Progress Report 1991, Villigen, Annex III, Annual Report, p. 68 (1992)

[3] M. Suzuki, J. M. Smith, Adv. Chromatogr. 13, 241 (1975)